

Nanoscopic Topology of Pyrex

J. C. Phillips¹ and R. Kerner²,

1. Dept. of Physics and Astronomy, Rutgers University, Piscataway, N. J., 08854-8019

2. LPTMC, University Pierre et Marie Curie -CNRS UMR 7600, 75005 Paris, France

Abstract

Window glass is a ternary mixture, while pyrex (after window glass, the most common form of commercial glass) is a quaternary. Building on our previous success in deriving the composition of window glass without adjustable parameters, and borrowing from known reconstructed crystalline surfaces, we model pyrex as silica clusters with a specific ternary interface. This structure is consistent with the optimized resistance of pyrex to mechanical and thermal shocks, and it suggests new directions for studying the nanoscopic structure of this remarkable material.

In principle the structure of glasses is an exponentially complex combinatorial problem. In the early days of glass science it was customary to dismiss this problem by saying that network glasses, for example, form “continuous random networks”, or that metallic glasses could be modeled by “random” packing of hard spheres. Modern glass theory goes far beyond these early models, but there are still many approaches to understanding glass structure and properties. One approach, that has the advantage of being close to commercial practice, is variational (standard for mathematical studies of non-polynomial complete (complex) problems) and focuses attention on optimizing structural properties. Here we adopt this approach to study pyrex (next to window glass, this is the most common form of commercial glass), using the methods of surface science to study internal interfaces.

Borosilicate glasses mix tetrahedrally disposed $\text{Si}(\text{O}_{1/2})_4$ with ring-disposed $\text{B}_2\text{O}_3 = [(\text{BOO}_{1/2})_6]/3$, raising an interesting question: is it possible to characterize the network properties of borosilicates topologically? Topology is a powerful tool for analyzing the structure of network glasses, as proved by the derivation of the ternary composition of window glass [74% SiO_2 , 16 % Na_2O , 10% CaO] without using adjustable parameters, as shown in Fig. 1; see [1] for details. The central reason for the success of the topological approach to the structures of network glasses is that optimized glassy networks are stress-free [2] and fill space maximally according to rules obtainable from crystal chemistry [3]. These rules by themselves are incomplete (for instance, they are incapable of distinguishing quantitatively between corner-sharing and edge-sharing tetrahedra), but when combined with experimental data (Raman, NMR, etc.), theory often confirms optimal compositions within a few % (practically exact for many cases, including window glass). Thus it appears that topology is indeed a long-sought “royal road” to understanding the structures and compositions of optimized network glasses [4].

Borosilicate glasses are of growing interest, especially for nuclear waste encapsulation [5,6], but they are already familiar both within and without laboratories, as pyrex is an optimized borosilicate glass, selected in 1915 from thousands of compositions for its optimized ability to sustain mechanical shock [7]. The ability to resist thermal shock depends on thermal expansivity, and because of thermal fluctuations during quenching there is a good correlation between the two abilities to resist shock [8]. However, we will also find that this correlation has a firm nanoscopic basis, which is important for commercial optimization, and may well be especially significant for small carefully quenched samples.

When glasses are quenched from the melt, they usually have larger volumes than the weighted molar volumes of their crystalline constituents. This “free volume” is normally distributed in the form of thin internal surface layers of lower density separating nanoclusters. In the case of ternary window glass [74% SiO_2 , 16 % Na_2O , 10% CaO] [1], it was possible to ignore the internal surfaces, and to treat the network (see Fig. 1) as a

stress-free mixture M with an average number of rings passing through each cation of $R = 6$ (just as in pure silica). The (invalid for most silicates) assumption {"prediction"} [1] that the distribution of cations in soda lime silicate glasses is nearly homogeneous ("random") near the optimized composition of window glass has since been supported by NMR experiments [9], which also showed evidence for local Na-Ca pairing, in agreement with Fig. 2 of [1]. However, the shock resistance of quaternary pyrex (80.6%SiO₂, 13.0%B₂O₃, 4.1%Na₂O, 2.3%Al₂O₃) empirically requires that these internal surfaces be chemically strengthened by the elimination of CaO (cation valence $Z = 2$), as well as replacement of $\frac{3}{4}$ of the Na₂O (cation valence $Z = 1$) by B₂O₃ (cation valence $Z = 3$), the addition of some silica (cation valence $Z = 4$), and even the replacement of 3% of the silica by Al₂O₃ (cation valence $Z = 3$, very refractory, higher melting point (2000C) than silica (1700C)). This is all very well, but how can these larger Z elements be added to the network without producing a large internal pressure, whose fluctuations would amplify external stresses, thus producing undesirable mechanical or thermal failure?

This problem is typical in the optimization of materials – when one has a material (such as ternary window glass) whose properties already appear to be optimized, it seems that any attempt at further optimization is self-defeating. The proposed solution for pyrex is sketched in Fig.2. Silica nanoclusters are formed in the melt, and their interfaces are decorated with Na₂O and B₂O₃. To understand the interfacial stress, it is helpful to compare pyrex to the simple prototypical binary $(\text{Na}_2\text{O})_x(\text{SiO}_2)_{1-x}$, whose phase diagram has been very well studied [1]. The reduction in network constraints (softening, reduction of T_g) by the addition of Na₂O (average number of resonating bonds $\langle R \rangle = 4/3$) to silica ($\langle R \rangle = 8/3$) is compensated by addition of oxygen bond-bending constraints, so that $(\text{Na}_2\text{O})_x(\text{SiO}_2)_{1-x}$ forms a stress-free network between $x = 0$ and $x = 0.20$ [1,10], with the glass transition temperature T_g decreasing rapidly with x . In this simple binary Na₂O covers the cluster interfaces (right half of Fig.1).

In pyrex on the opposing face of the neighboring cluster, we replace Na_2O and several (~ 2) layers of SiO_2 by B_2O_3 . Pyrex contains ~ 3 times as many B_2O_3 molecules as Na_2O . The “extra” B_2O_3 is probably used to build inner “healing” layers of B_2O_3 ; these could contain a large fraction of tetrahedral $\text{B}(\text{O}_{1/2})_4$, as NMR has shown that these occur in borosilicates [11] (tetrahedra pack better than rings, and here the $\text{B}(\text{O}_{1/2})_4$ tetrahedra pack well with silica tetrahedra). In any case, the “healing” layers terminate with a surface monolayer of $\text{O}_{1/2}\text{-B}=\text{O}$ (non-bridging O). If we fuse $\text{B}=\text{O}$ into a single cation, then this surface layer is topologically isomorphic to $\text{O}_{1/2}\text{-Na}$.

In Fig. 2 two (not just one) things favorable for shock resistance happen: first, the outer left oxygen anions are attracted electrostatically by the outer right Na cations, and second, interfacial stress is minimized, because the molar volumes of B_2O_3 and Na_2O [which fix the respective length scales] are virtually identical (as are their molecular masses, which means that there is also little temperature dependence to the lateral misfit strain energy). In reduced units the crystalline molar volumes are: SiO_2 (cristobalite) = 1.00, Na_2O = 1.05, B_2O_3 = 1.09, and Al_2O_3 = 0.99. Of course, one can say that the approximate matching of the molar volumes of B_2O_3 and Na_2O is “accidental”, but when a certain quaternary composition is selected from thousands of alternatives, it is just such “accidents” that are needed. Alternatively, what we have here is a kind of evolutionary selection by “trial and error”, and such empirically optimized selection is hardly ever accidental.

We now discuss details of the model. For simplicity both silicon subnetwork surfaces in Fig. 2 are drawn in (100) crystalline orientation, but in the glass one expects a distribution of orientations, which should be averaged over. After such an average over orientations, scalar factors (specifically, molar volume differences) should dominate internal network interfacial (both hydrostatic and shear) misfit energies. Moreover, the interfacial structure shown in Fig. 2 refers specifically to an optimized composition near 80% silica. Thus the dominance of (1B,3Si) over (2B,2Si) in tetrahedral $^{[4]}\text{B}$ in a 55%

silica alkali borosilicate environment [12], together with a larger concentration of $^{[3]}B$ in rings, merely reflects ring-tetrahedra nanoscale phase separation, with (1B,3Si) $^{[4]}B$ interfaces with (111) oriented silica interfaces. Note that the matched interfaces in Fig. 2 (80% silica) will be stabilized primarily by longitudinal (not shear) forces, which is another way of saying that the selected configuration of pyrex can be exceptionally stable both mechanically and thermally. Conversely, opposing ionic interfaces covered only by Na_2O (as in $(Na_2O)_x(SiO_2)_{1-x}$) will experience isotropic Coulomb repulsive forces, with substantial shear components, and larger thermal and mechanical instabilities.

Just as the $d = 3$ silica clusters are separated by $d = 2$ internal interfaces, so stress accumulation (or alternatively, quenching kinetics) separates the $d = 2$ internal interfaces into patches separated by $d = 1$ line segments. Refractory alumina edge-sharing tetrahedral chain segments presumably reinforce these edges, thereby further enhancing pyrex's ability to sustain mechanical or thermal shock. Quite generally one can argue that in an isotropic medium $(surface/volume) \sim (line/surface)$; this relation can be used to place limits on the Al_2O_3 concentration. An upper limit f_2 is obtained if "surface" is interpreted to mean all components except silica, so that $(surface/volume) \sim 0.2$, giving $f_2 \sim 4\%$. Alternatively, one could include only the outer B_2O_3 and Na_2O layers, so that $(surface/volume) \sim 0.1$, giving a lower limit $f_1 \sim 1\%$. The actual value for Al_2O_3 in pyrex is 2.3%, comfortably between f_1 and f_2 .

We can gain further insight into the structure of pyrex by analyzing the results of a mean-field model with modest correlations, similar to the window glass model [1]. We can look upon the pyrex network as being composed of four elementary building blocks: $Si(O_{1/2})_4$ [A], $B(O_{1/2})_3$ [B] $Na(O_{1/2})$ [C], and $Al(O_{1/2})_3$ [D]. Only the A-block represents an equivalent of one SiO_2 molecule, while the other three (B,C and D blocks) represent only halves of corresponding molecules. This is why the concentrations of these blocks, denoted by p_A , p_B , p_C and p_D are not the same as the chemical composition denoted by $(1-x-y-z)$, x , y and z , respectively. If the total number of molecules is N , then the

numbers of various blocks will be: $N(1-x-y-z)$ (for the A blocks), $2Nx$ (for the B blocks), $2Ny$ (for the C-blocks), and $2Nz$ (for the D-blocks), because each molecule (except for SiO_2) gives rise to **two** building blocks. Therefore the concentrations of blocks A,B,C and D can be expressed as functions of chemical concentrations $(1-x-y-z)$, x, y and z as follows: $\mathbf{p}_A = (1-x-y-z)/(1+x+y+z)$, $\mathbf{p}_B = 2x/(1+x+y+z)$, $\mathbf{p}_C = 2y/(1+x+y+z)$, and $\mathbf{p}_D = 2z/(1+x+y+z)$. For the pyrex composition (80.6% SiO_2 , 13.0% B_2O_3 , 4.1% Na_2O and 2.3% Al_2O_3) the corresponding block concentrations will be: $\mathbf{p}_A = 67.5\%$, $\mathbf{p}_B = 21.8\%$, $\mathbf{p}_C = 6.9\%$, and $\mathbf{p}_D = 3.8\%$.

In order to fix the optimal values of concentrations (x,y,z) one needs three independent equations. One of the three equations can be readily derived from the maximal topological homogeneity applied to the ring structure, i.e. the medium-range order, as in window glass [1]. There the reduction in average number of rings due to Na creating non-bridging oxygens is compensated by refractory Ca “zipping together” the silica rings attached to it, increasing the number of rings by 15. Here a similar count for Al-centered tripods “zipping together” surrounding A-blocks creates 30 excess rings created around each D-block. Supposing that each B-block behaves in fact in the same way as a C-block i.e. “eats out” one of the oxygen bonds stemming from an A-block (Si-centered tetrapode), thus reducing the number of rings by three, one should have 10 times as many B and C blocks taken together as the D-blocks: $(\mathbf{p}_B + \mathbf{p}_C) = 10 \mathbf{p}_D$. This equation is roughly satisfied: we have $(\mathbf{p}_B + \mathbf{p}_C) = 28.7\%$ and $\mathbf{p}_D = 3.8\%$. [This is one of the places where the interfacial model of Fig.1 is helpful: it shows that the D Al_2O_3 blocks play a different structural role than the B (B_2O_3) and C (Na_2O) blocks, so the equation should not be satisfied exactly. Note, however, that this equation also explains why the D Al_2O_3 blocks have such a large effect on the network, even though their concentration is small.]

Another equation can be produced if we take into account topological equilibrium between tetrapods and tripods. The B and C blocks transform the A-blocks (the Si-centered tetrapods often called Q_4 in publications discussing silicate glasses) into tripods

(denoted by Q_3). Now, it is reasonable to assume that the Q_4 and Q_3 entities should not concentrate too much – they should “dilute” as homogeneously as possible, avoiding local pairing of one or another type. Supposing that each B or C block transform exactly one Q_4 into a Q_3 , we conclude that out of $(1-x-y-z)$ A-blocks there will be $(2x + 2y)$ transformed into Q_3 blocks (with one neutralized oxygen bond out of four). If we assume that as a result, each Q_3 block is surrounded by three Q_4 blocks, avoiding direct contact between two Q_3 ‘s and that each Q_4 block is surrounded by four Q_3 ‘s, we arrive at the stoichiometric ratio $\frac{3}{4}$. This leads to the following equation:

$$4(1 - 2 p_B - 2 p_C - 3 p_D) = 3(p_B + p_C)$$

The third equation can be derived from the rigidity theory. Supposing that the action of Na_2O eases the constraints by suppressing 3 constraints per one $Na+O$ Group (one broken bond and two broken angular constraints), whereas the action of B_2O_3 via the formation of doubly bonded oxygens creates an extra constraint, we arrive at the relation

$$p_B = 3 p_C$$

Together with the remaining two equations expressed by means of the variables

p_A , p_B , p_C and p_D we get the following system:

$$p_A + p_B = 10 p_C$$

$$p_B = 3 p_C$$

$$4(1 - 2 p_B - 2 p_C - 4 p_D) = 3(p_B + p_C)$$

whose solution is: $p_A = 0.650$ [0.675], $p_B = 0.239$ [0.218], $p_C = 0.079$ [0.069] and $p_D = 0.032$ [0.038], which agrees well with the real values [in brackets]. However, the special property of pyrex- excellent thermal and mechanical stability, unlike $(Na_2O)_x(SiO_2)_{1-x}$, requires the special interfacial attraction illustrated in Fig.1.

Because the number of possible compositions is so large, the data base for most glasses (apart from silica-soda-lime, that is, window glass) is sparse and fragmentary. Our variational approach, together with our interfacial structural model, suggests promising new directions for fundamental studies of glass structure. It should not be difficult to expand the pyrex-like data base, with three-point (parabolic) composition meshes,

varying each component separately, while retaining fixed proportions for the remaining components, thus: SiO_2 , (80±5)%., B_2O_3 , (13±3)%., Na_2O , (4±2)%., and Al_2O_3 , (2.5±1)% (only 9 compositions, including pyrex, for a quaternary mixture). Many macroscopic parameters could be measured, but density, T_g , and especially thermal expansivity [seldom measured] are all important, as well as elastic constants [10]. At the microscopic level the doubly bonded interfacial B is unlikely to produce an observable NMR signal, but it is quite possible that the tetrahedral $^{[4]}\text{B}$ populations [11,12] could exhibit a large non-linearity in composition (possibly a bulge, or even a peak) near the pyrex composition. Further progress in understanding pyrex may be obtained by extending earlier work on $^{[4]}\text{B}$ in a 55-65% silica alkali borosilicate environment [12] to the pyrex neighborhood of 80% silica, and testing our idea that a proper balance between $^{[3]}\text{B}$ and $^{[4]}\text{B}$ populations can minimize thermal expansivity and maximize shock resistance.

In conclusion, we have proposed a new structural model for pyrex (next to window glass, the most common form of commercial glass), and suggested new experimental directions. The unique properties of pyrex, which have led to its enormous practical successes, are modeled as the result of optimization of internal interfaces and edges between silica-like nanoclusters [13]. Many alternative structural models of glasses are non-variational in nature, and rely on nucleation concepts that idealize the glass transition as nearly first-order. These models involve mean-field concepts (such as surface tension) that are not easily quantified chemically. Our model, which focuses on the variational properties of stress-free, or stress-minimized networks, readily leads to specific chemical models. In the case of window glass, the mean field equations are essentially exact, while they predict the composition of pyrex with errors of ~ 2%. It is just these very small differences that require a designed cluster model and are responsible for the distinctive physical properties of pyrex. Moreover, network models are of great interest as paradigms of possible approaches to exponentially complex problems in general, in fields as far removed as high temperature superconductivity [14] and solvability of large-scale Boolean algebras in computer science [15-17].

We are grateful to K. Rabe for a stimulating conversation.

References

1. R. Kerner and J. C. Phillips, Solid State Comm. **117**, 47 (2000).
2. S. Chakravarty, D. G. Georgiev, P. Boolchand, and M. Micoulaut, J. Phys. Cond. Mat. **17**, L1 (2005).
3. J. C. Phillips, J. Non-Cryst. Sol. **34**, 153 (1979); **43**, 37 (1981).
4. W. D. Kingery, *Introduction to Ceramics* (Wiley, New York, 1976), pp. 120, 765.
5. I. A. Sobolev, S. A. Dmitriev, F. A. Lifanov, *et al.*, Glass Tech. **46**, 28 (2005).
6. M. I. Ojovan, R. J. Hand, N. V. Ojovan, *et al.*, J. Nuc. Mat. **340**, 12 (2005).
7. W. B. Jensen, J. Chem. Ed. **83**, 692 (2006).
8. N.P. Bansal and R.H. Doremus, *Handbook of Glass Properties* (Academic Press, New York, 1986).
9. S. K. Lee and J. F. Stebbins, J. Phys. Chem. B **107**, 3141 (2003).
10. Y. Vaills, T. Qu, M. Micoulaut, *et al.*, J. Phys.-Cond. Matt. **17**, 4889 (2005).
11. L. S. Du, J. R. Allwardt, B. C. Schmidt, *et al.*, J. Non-Cryst. Sol. **337**, 196 (2004).
12. L. S. Du and J. F. Stebbins, J. Non-Cryst. Sol. **315**, 239 (2003).
13. F. Leonforte, A. Tanguy, J. P. Wittmer, and J.-L. Barrat, Phys. Rev. Lett. **97**, 055501 (2006).
14. P. Boolchand, G. Lucovsky, J. C. Phillips, and M. F. Thorpe, Phil. Mag. **85**, 3823 (2005).
15. R. Monasson, R. Zecchina, S. Kirkpatrick, B. Selman, and L. Troyansky, Nature **400**, 133 (1999).
16. G. Biroli, R. Monasson, and M. Weigt, Europ. Phys. J. B **14**, 551 (2000).
17. S. Cocco and R. Monasson, Theo. Comp. Sci. **320**, 345 (2004).

Figure Captions

Fig. 1. Topological derivation of the composition of window glass. The mean-field (stress-free) condition is represented by the line M, while the ring condition is represented by the line R. The two lines intersect at W, the composition of window glass. See [1] for details.

Fig. 2. Suggested interfacial structure for pyrex-like $\text{SiO}_2 - \text{B}_2\text{O}_3 - \text{Na}_2\text{O}$ interface. The network structure near the interface exhibits several favorable features that would optimize the mechanical shock resistance and minimize thermal expansivity of the glass.

Fig. 1.

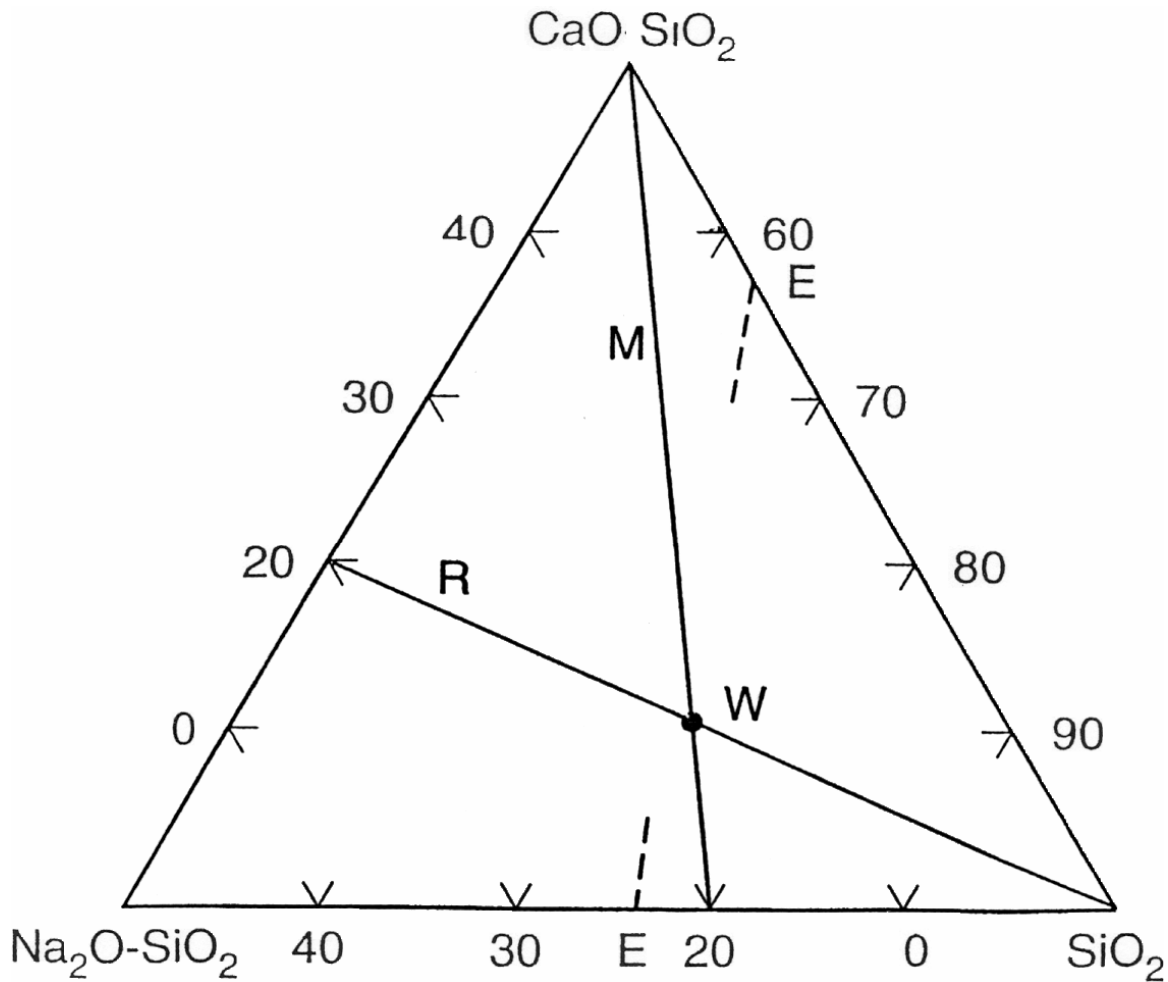


Fig. 2.

